Combined inhibition of insulin growth factor 1 receptor and autophagy prevents colorectal cancer metastasis.

MAHGOUB, Eglal, BAJBOUJ, Khuloud, AHMED, Samrein <http://orcid.org/0000-0001-9773-645X>, HAFEZI, Shirin, ELDOHAJI, Leen, VENKATACHALAM, Thenmozhi, HACHIM, Mahmood, AL HAMIDI, Tasneem, SHAFARIN, Jasmin, ABDEL-RAHMAN, Wael M, SULAIMAN, Nabil, HAMOUDI, Rifat, TANEERA, Jalal, LAKHTAKIA, Ritu, TALAAT, Iman M and SABER-AYAD, Maha

"Combined Inhibition of Insulin Growth Factor 1 Receptor and Autophagy prevents Colorectal Cancer Metastasis"

Eglal Mahgoub[1,2], Khuloud Bajbouj[§1,2], Samrein Ahmed[§3], Shirin Hafezi[2], Leen Eldohaji[2], Thenmozhi Venkatachalam[4], Mahmood Hachim[5], Tasneem Al Hamidi[2], Jasmin Shafarin[2], Wael M. Abdel-Rahman[2,6], Nabil Sulaiman[1,7,8], Rifat Hamoudi[1,2,9,10], Jalal Taneera[1,2], Ritu Lakhtakia[5], Iman M. Talaat[1,2,11], Maha Saber-Ayad[1,12]

[1]College of Medicine, University of Sharjah, Sharjah 27272, United Arab Emirates

[2]Research Institute of Medical and Health Sciences, University of Sharjah, Sharjah 27272, United Arab Emirates

[3]College of Health, Wellbeing and Life Sciences, School of Biosciences and Chemistry, Biomolecular Sciences Research Centre, Sheffield Hallam University, Sheffield S1 1WB, United Kingdom.

[4]Khalifa University, Abu Dhabi, United Arab Emirates.

[5]College of Medicine, Mohammed bin Rashid University of Medicine and Health Sciences, Dubai, United Arab Emirates.

[6]Department of Medical Laboratory Sciences, College of Health Sciences, University of Sharjah, Sharjah, United Arab Emirates.

[7]Baker Heart and Diabetes Institute, Melbourne, Victoria, Australia.

[8]University of Melbourne, Melbourne, Victoria, Australia.

[9]Division of Surgery and Interventional Sciences, University College London, London, United Kingdom

[10] BIMAI-Lab, Biomedically Informed Artificial Intelligence Laboratory, University of Sharjah, Sharjah P.O. Box 27272, United Arab Emirates.

[11]Faculty of Medicine, Alexandria University, Alexandria, 21131, Egypt.

[12]Faculty of Medicine, Cairo University, Giza, Egypt.

*** Correspondence:**

msaber@sharjah.ac.ae

§ Equal contribution

Keywords: Autophagy, Colorectal Cancer (CRC), EMT Markers, Metastasis, Insulin-Growth Factor Receptor (IGF-1R).

Abstract

The role of Insulin-like growth factor 1 (IGF-1) in promoting cancer proliferation has been identified, yet its potential role in metastasis has not been fully elucidated. Autophagy plays a pivotal, yet controversial, role in regulating cancer cell behaviour. Our previous transcriptomic analysis identified autophagy-related genes and insulin-like growth factor 1 receptor (IGF-1R) among the most differentially expressed in advanced versus early-stage colorectal cancer (CRC). In this study, we investigated the functional interplay between IGF-1R signalling and autophagy in CRC progression and metastasis, using a panel of CRC cell lines, including HCT116 cells with targeted CRISPR-Cas9 knockout of ATG5 and ATG7.

Our results demonstrate that stimulation with IGF-1 enhances autophagic flux, whereas IGF-1R knockdown suppresses autophagic activity. Notably, dual inhibition of IGF-1R and autophagy led to a marked reduction in CRC cell migration and invasion. In ATG5-/- and ATG7-/- cells, IGF-1R silencing significantly downregulated mesenchymal markers Vimentin, Slug, and Snail, while upregulating the epithelial marker E-cadherin. Additionally, combined inhibition resulted in increased size and number of focal adhesion molecules, such as paxillin and zyxin.

Collectively, these findings highlight the synergistic effect of IGF-1R and autophagy inhibition in suppressing EMT and metastatic potential in CRC cells, suggesting that this combinatorial approach may represent a promising therapeutic strategy for metastatic CRC.

Graphical abstract:

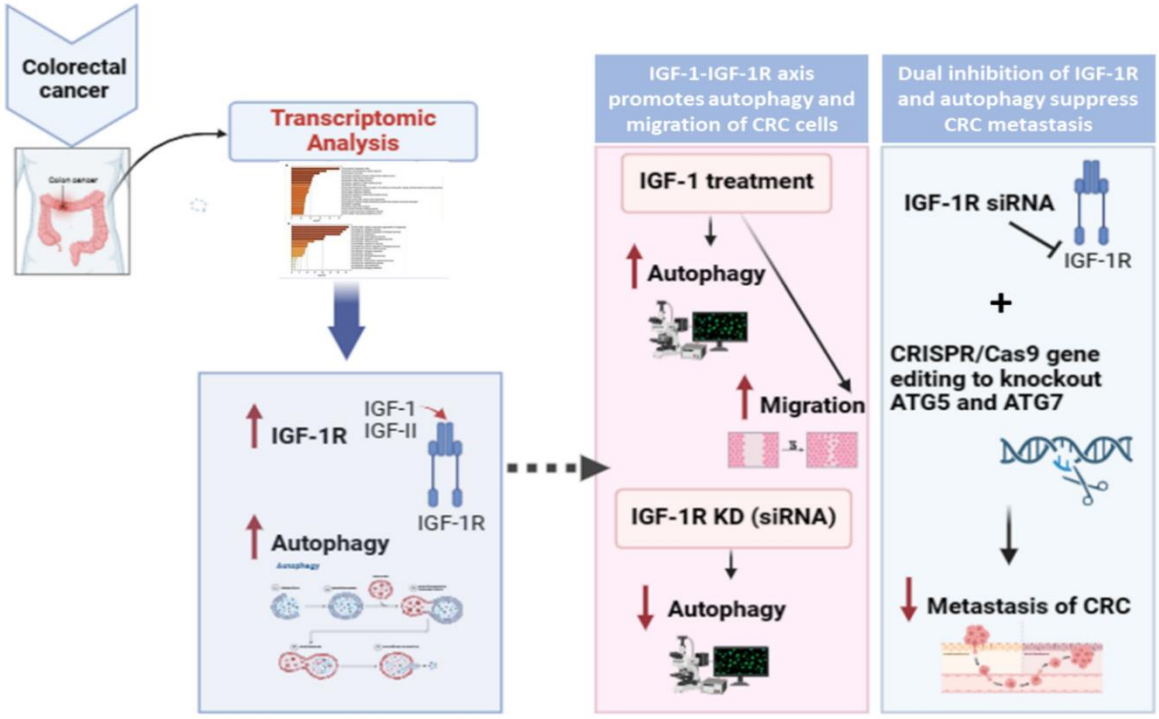

Abbreviations:

IGF1: Insulin growth factor 1; IGF-1R: insulin growth factor 1 receptor; PI3K: Phosphatidylinositol 3-kinase; mTOR: Mammalian target of rapamycin; MAPK: Mitogen-activated protein kinase; VEGFR: Vascular Endothelial Growth Factor Receptor; LC3B: Autophagy protein microtubule-associated protein 1 light chain-3B; ATG5: Autophagy Related 5; ATG7: Autophagy Related 7; SQSTM1/p62: protein Sequestosome 1; EMT: Epithelial-mesenchymal transition; MRP-1: multidrug resistance-associated protein-1; 3-MA: 3-Methyladenine.

Introduction

CRC ranks third in prevalence among all cancers and second in causes of cancer death worldwide [1]. The incidence of the disease has been found to vary significantly among populations [2]. The occurrence of (micro)metastasis drastically worsens the prognosis [3].

Autophagy, a key degradative process essential for cellular adaptation, has dynamic roles in cancer initiation, progression, and treatment response [4-6]. In rapidly growing tumors exposed to hypoxia and nutrient deprivation, autophagy provides metabolites and energy required for survival [7, 8]. In addition, epithelial-mesenchymal transition (EMT), a crucial mechanism for cancer cell invasiveness and metastasis, has been linked to autophagy in the context of cancer cell metastasis [9, 10].

Metabolic syndrome, a chronic inflammatory condition, has been associated with increased risk and progression of cancers, including CRC [11, 12]. IGFRs are physiologically expressed in the muscular and mucosal layers of the colon surfaces, and their expression is significantly elevated in CRC [13]. Dysregulation of the IGF–IGF-1R axis represents a key mechanistic link between metabolic syndrome and cancer, influencing proteins involved in apoptosis and autophagy and contributing to enhanced cell survival [14].

IGF-1R signaling pathway significantly affects the crosstalk between DNA damage and inflammation. IGF-1R is a cell surface receptor that binds to insulin and IGF-1, two hormones that promote cell growth and survival [15]. It has been shown that high insulin levels are associated with cancer development and progression through the IGF-IGF-1R axis [16]. IGF-1R signaling regulates autophagy through IRS1-mediated activation of the PI3K–Akt–mTOR pathway [17, 18].

Previous findings further revealed that IGF-1R fragments co-localize with LC3-II and activate ShcA within dense organelles, after which both proteins are sequestered into phosphorylated autophagic vacuoles for degradation [19]. Through ShcA, IGF-1R also signals via the MAPK pathway to promote proliferation. Although activation of the IGF–IGF-1R axis is well recognized in cancer progression, its contribution to CRC migration and metastasis remains incompletely understood.

In a previous study [20], utilizing transcriptomics analysis in CRC cases ranging from TNM stages I to IV, IGF-1R was identified as the top upregulated gene in late CRC (TNM II and III) compared to early-stage I. Additionally, we identified autophagy as one of the top five differentially regulated pathways, implicated as a driver for tumor progression in late CRC stages. In light of these findings, it is of interest to explore the link between IGF-1R and autophagy in CRC migration and invasion.

Our current study revealed that IGF-1 promotes autophagy in CRC cells, thereby facilitating migration and metastasis. Intriguingly, we also observed that simultaneous inhibition of both the IGF-IGF-1R axis and autophagy holds promise as a potential adjuvant therapy to prevent and/or suppress metastasis in CRC effectively.

Methods

1) CRISPR/Cas-9 gene Editing.

- **Design and Transfection:**

A ribonucleotide protein has been used [21] as a delivery system for CRISPR-mediated knockout targeting autophagy-related gene 5 (ATG-5) and ATG-7 within HCT116 cells. All necessary reagents were procured from Thermo Fisher Scientific, USA. Two guide RNAs (gRNAs) were utilized individually to target the ATG5/7 genes. Lipofectamine™ CRISPRMAX™ Cas9 Transfection Reagent facilitated the transfection of cells with both gRNAs and Cas9 protein. Genomic cleavage efficiency was evaluated via immunoblotting specific to the desired genes. Throughout the experimental procedure, TrueGuide™ sgRNA Positive Control, CDK4 served as a positive control to validate the methodology.

- **Validation and Clone Selection:**

A scrambled gRNA, TrueGuide gRNA negative control, was employed as a negative control to ensure the specificity of the target. The cell pool exhibiting the highest transfection efficiency was selected for downstream validation. To generate isolated clones with a complete knockout, the mixed cell pool was diluted to 1 cell/200µl in a liquid medium and then seeded into 96-well plates to facilitate the formation of individual clones. These clones were subsequently subjected to immunoblotting to assess the expression of ATGF5/7, confirming the success of the knockout procedure.

2) Cell lines and Treatment Protocol.

- **Cell lines:**

A panel of cell lines representing different stages of colorectal cancer was utilized in this study, including HCT116, HT29, and NC (negative control cells that were used during the CRISPR/Cas9 gene editing experiments), LoVo, and SK-CO-1. HCT116 (CCL-247EMT), HT29 (HTB-38), LoVo (CCL-229), and SK-CO-1 (HTB-39) cell lines were obtained from American Type Culture Collection (ATCC, Manassas, VA, USA). HCT116 cell lines harboring knockout mutations for ATG5 and ATG7 were generated using CRISPR/Cas9 methodologies, following established protocols.

- **Culture Condition:**

Cell cultures were maintained at 37°C in a humidified atmosphere containing 95% air and 5% CO2. LoVo and SK-CO-1 cell lines were cultured in Dulbecco's Modified Eagle's Medium Nutrient Mixture F-12 Ham, while the remaining cell lines were sustained in RPMI Media. Both media formulations were supplemented with 10% fetal bovine serum and 1% antibiotics (penicillin/streptomycin). Cells were cultivated in 75-cm2 tissue culture flasks and subjected to regular sub-culturing every 3-4 days using trypsin, with continued incubation in a humidified incubator set at 37°C with 5% CO2 and 95% room air.

- **Drug Treatment:**

For the experimental treatment, cells were seeded in T25 flasks at a density of 1 million cells per flask. They were treated with 10 nM of Bafilomycin A1 (Cat. No. HY-100558-5mg, Medchem Express) and 10 nM of IGF-1 [22] (Sigma Aldrich, Cat. No. I3769-50UG) for 24 hours. Untreated cells served as the control group.

3) Transfection siRNA.

All panels of CRC cells (HCT116, HT29, LoVo, SK-CO-1, HCT116 ATG5-/-, HCT116 ATG7-/-) were seeded in a 6-well plate with a range of 200,000 to 600,000 cells per well in antibiotic-free medium. The next day, the cells were transfected with 50nM of ON-TARGET plus SMARTpool siRNA/well-targeting IGF-1R (Cat. No. L -003012-0005, Dharmacon) in the presence of lipofectamine RNAiMAX solution (Cat. No. 13778075, Thermo Fisher Scientific) following the manufacturer's instructions. A scrambled siRNA was used as a control. Cells were collected for protein and RNA extractions 48 hours post-transfection.

4) Quantitative real-time polymerase chain reaction (qRT-PCR).

- **RNA Extraction and cDNA Synthesis:**

According to the manufacturer's instructions, total RNA was isolated using the Invitrogen™ PureLink™ RNA Mini Kit. The extracted RNA was subsequently reverse transcribed into cDNA utilizing the SensiFAST™ cDNA Synthesis Kit. The primers are listed in Table 1.

- **Amplification:**

Quantitative real-time PCR was performed on a QuantStudio 3 system (Thermo Scientific) with the SensiFAST™ SYBR Hi-ROX kit. Each sample was analyzed in triplicate. Mean threshold cycle (Ct) values were determined for each gene, and relative gene expression was calculated using the $2(-\Delta\Delta C(T))$ method.

Table 1. List of primer sequences used in qPCR.

Genes	Forward primer sequence	Reverse primer sequence
LC3B	GAACGGACACAGCATGGTCAGC	ACGTCTCCTGGGAGGCATAG
P62	TTGTACCCACATCTCCCGCCA	TACTGGATGGTGTCCAGAGCCG
E-cadherin	ATTTTTCCCTCGACACCCGAT	TCCCAGGCGTAGACCAAGA
Vimentin	AGTCCACTGAGTACCGGAGAC	CATTTCACGCATCTGGCGTTC
Snail	ACCACTATGCCGCGCTCTT	GGTCGTAGGGCTGCTGGAA
GAPDH	TGTTGCCATCAATGACCCCTT	CTCCACGACGTACTCAGCG

5) Immunofluorescence.

- **Cell Fixation and permeabilization:**

CRC cells were plated onto coverslips in 6-well plates and allowed to adhere for 24 hours. Following cell treatments, cells were fixed with 4% paraformaldehyde at room temperature for 10 minutes. Subsequently, the fixed cells underwent blocking for one hour at room temperature in PBS containing 2% BSA, followed by permeabilization for 15 minutes using 0.1% Triton X-100.

- **Primary and Secondary Antibodies Incubations:**

The anti-LC3 antibody (Cat. No. 18725-1-AP, Proteintech) (diluted 1:200 in PBS with 2% BSA) was then applied to the cells and allowed to incubate overnight at 4 °C. After a PBS wash, the cells were subjected to a one-hour incubation at room temperature with an Alexa Fluor 488-conjugated anti-Rabbit antibody (diluted 1:500 in PBS with 2% BSA; Molecular probe, Invitrogen, Carlsbad, CA, USA).

Primary antibodies anti-Paxillin (1:300, Cat. No. 10029-1-IG, Proteintech) and anti-Zyxin (1:300, Cat. No. ab58210, Abcam) were incubated overnight at 4°C. After a PBS wash, the cells were subjected to a one-hour incubation of a mixture of secondary antibodies at room temperature in the dark.

- **Imaging and Analysis:**

To visualize the cells, a confocal microscope was employed for mounting and examination of the slides. For the analysis, Image J software from the National Institutes of Health [23], was utilized.

6) Wound healing Assay (Cell Migration Assay).

This assay was employed to assess the migration of the previously described CRC cell lines, which were knocked out for IGF-1R using siRNA as well as treatment with IGF-1.

The cells were plated in 12-well dishes with 3 mL of media. The wound was created in the center of each well by scratching the culture plate with a pipette tip. The debris was subsequently washed with PBS. The migration of the cells was observed for 0 and 48 hours following IGF-1 treatment and IGF-1R transfection. As a control, a well with only cells and liquid was included. To quantitatively analyze the cell movement, Image J software from the National Institutes of Health, was utilized.

7) Western Blot.

- **Protein Extraction, Electrophoresis, and Transfer:**

RIPA lysis buffer was used for protein extraction (Cat. No. ab156034, Abcam). The protein concentration in the cell lysate was measured using a BCA kit (Pierce) following the manufacturer's instructions (Cat. No. 23227, Thermo Scientific Pierce, Waltham, MA, USA). A volume equivalent to 35µg of total protein was separated on 10% sodium dodecyl sulphate-polyacrylamide gel electrophoresis (SDS-PAGE) that was then electrophoretically transferred to PVDF membrane (Bio-Rad, USA). The membrane was blocked for one hour at room temperature using 5% BSA powder.

- **Antibody Incubation:**

Following blocking, the membrane was washed with TBST and incubated overnight at 4°C with primary antibodies, including anti-IGF-1R (Cat. No. D406W), anti-LC3B (Cat. No. 83506), anti-ATG5 (Cat. No. 12994S), anti-ATG7 (Cat. No. 8558S), anti-P62 (Cat. No. 39749S), anti-β-actin (Cat. No. 4970S) (all from Cell Signaling Technology, Danvers, MA, USA), overnight at 4 °C. Secondary antibodies (Cell Signaling Technology, Danvers, MA, USA) were incubated with the membrane for 1 hour at room temperature at a ratio of 1:1000.

- **Detection and Quantification:**

The ECL kit (Thermo Scientific Pierce, Waltham, MA, USA) was used to identify chemiluminescence to identify and quantify protein bands, Bio-Rad Image Lab software (ChemiDocTM Touch Gel and Western Blot Imaging System; Bio-Rad, Hercules, CA, USA) was used. Protein levels were normalized to β-actin, and ratios were calculated based on the values of control samples.

8) Flow cytometry analysis.

The expression levels of EMT markers, -E-cadherin, vimentin, and Slug, were assessed by flow cytometry. Cells were collected and washed with cold FACS buffer (PBS containing 2% FBS and 0.1% sodium azide), followed by permeabilization with Cytofix solution for Slug, then incubated with rabbit monoclonal antibodies against E-cadherin, vimentin, or Slug (EMT sampler kit Cat. No. 9782T, Cell Signaling Technology, Danvers, MA, USA). Following a 45-minute incubation at 4°C, cells were washed with FACS buffer and then incubated with a secondary Anti-rabbit IgG (Alexa Fluor® 488-conjugated) antibody. The cells were then washed twice with ice-cold PBS and analyzed on a BD FACSAria III flow cytometer (BD Biosciences, San Jose, CA, USA). Data acquisition was performed using BD FACS Diva software, and subsequent analysis was carried out with FlowJo software.

9) Matrigel Invasion Assay.

For the invasion experiments, 1×10^3 cells were introduced into the upper chambers of Transwells featuring an 8-µm pore size, which were pre-coated with Matrigel (Cat. No. 354480, Corning). The cells were suspended in RPMI-1640 media without fetal bovine serum (FBS) and added to the upper chambers, while the lower well was filled with 10% FBS RPMI-1640 medium. The entire setup was then incubated at 37°C in a 5% CO2 environment. After 24 hours of incubation, non-migrated or non-invaded cells were meticulously eliminated.

Subsequently, the cells on the filters underwent fixation with 4% paraformaldehyde, followed by permeabilization using 100% methanol. Staining of the filters was performed using 0.2% crystal violet. Analysis was carried out using an inverted microscope (Olympus Corp., Tokyo, Japan) at ×200 magnification, with five random fields counted per chamber for each membrane. The entire analysis procedure was repeated three times for robust results.

10) Bioinformatics.

GSCALite: Gene Set Cancer Analysis (GSCALite) is a web-based server that allows the exploration of gene expression patterns in datasets from cancer patients [24]. In this study, GSCALite was employed to investigate the role of IGF-1/IGF-1R in cancer-related pathways using the colon adenocarcinoma (COAD) dataset from The Cancer Genome Atlas (TCGA). The COAD-TCGA dataset included a total of 329 samples, comprising 288 tumor samples, 41 normal controls, and 26 paired samples. According to the dataset's analytical pipeline, samples were divided into two groups (High and Low) based on the median gene expression level. The difference in pathway activity score (PAS) between groups was assessed using the student's t-test, and the P value was adjusted by false discovery rate

(FDR) correction. An FDR ≤ 0.05 was considered statistically significant. When PAS (High expression of Gene A) > PAS (Low expression of Gene A), the gene was interpreted as having an activating effect on the pathway; otherwise, it was considered to have an inhibitory effect. This analysis provided insights into the potential regulatory role of IGF-1/IGF-1R in cancer-associated signaling pathways.

UALCAN: To analyze the expression of IGF-1R in normal tissues, different stages of tumors, and lymph node metastasis in CRC TCGA datasets, we utilized UALCAN. UALCAN is a web-based tool that utilizes OMICS data from various cancer datasets, including TCGA. Sample sizes for each group are indicated within the figure. Statistical significance was determined using Student's t-test [25].

GEPIA2: For the generation of overall survival Kaplan–Meier plots for IGF-1R in colorectal cancer (CRC) patients, we employed the Gene Expression Profiling Interactive Analysis 2 (GEPIA2) web-based server [26]. Sample sizes were n=135 for high IGF-1R expression and n = 135 for low expression. Statistical significance was evaluated using the log-rank (Mantel–Cox) test and hazard ratios (HRs) with 95% confidence intervals (CIs) were derived from Cox proportional-hazards regression analysis.

11) Statistics.

Graph Prism 8 (GraphPad Software Inc., La Jolla, California) was used to evaluate the significant results. Paired t-test was used to calculate p-values for comparisons between groups in each data set. The ANOVA test was used to compare more than two groups, and $p < 0.05$ was considered significant.

Results

1. The IGF-1-IGF-1R axis enhances autophagy flux and promotes migration in CRC cells.

In the first group of experiments, IGF-1R was efficiently silenced using siRNA in HCT116, HT29, LoVo, and SK-CO-1 cells 48 h after transfection, with knockdown efficiencies summarized in Supplementary Table 1 and representative protein reductions shown in S. Fig. S1A–D. Next, the effects of IGF-1 stimulation and IGF-1R knockdown on autophagy markers were first assessed at the mRNA level in HCT116, HT29, LoVo, and SK-CO-1 cells. IGF-1 significantly upregulated LC3B and downregulated P62 mRNA (Figure 1A, B), whereas IGF-1R silencing reduced LC3B and increased P62 mRNA expression (Figure 1C, D).

Consistent with these findings, western blot analysis showed that IGF-1 increased LC3B-II protein levels and decreased P62 protein abundance (Figure 1E), while IGF-1R knockdown reduced LC3B-I/II and elevated P62 protein levels (Figure 1F), indicative of impaired autophagosome formation. The quantitative summary of these effects across all cell lines is presented in Supplementary Table 2.

Immunofluorescence staining revealed an augmentation in LC3B puncta levels following IGF-1 treatment prior to bafilomycin A1(BafA1) compared to the untreated control group in CRC cell lines: HCT116, HT29, LoVo, and SK-CO-1 (Figure 1G). Moreover, using siRNA to target IGF-1R, we confirmed the previous results showing a substantial downregulation of LC3B puncta levels upon IGF-1R knockdown (Figure 1H). These findings further confirm the crucial functional role, at least in part, of the IGF-1-IGF-1R axis in modulating autophagy flux.

Next, the impact of IGF-1 treatment was determined on the migratory potential of CRC cells. Using similar panel of CRC cell lines, HCT116, HT29, LoVo, and SK-CO-1, wound healing assay was used to evaluate the influence of IGF-1 on cell migration. Our results demonstrate a significant increase in the migratory capacity of all CRC cell lines following treatment with IGF-1 (Figure 1I). These findings underscore the role of IGF-1 in facilitating migration, thereby implicating its potential contribution to the metastatic progression of CRC cells.

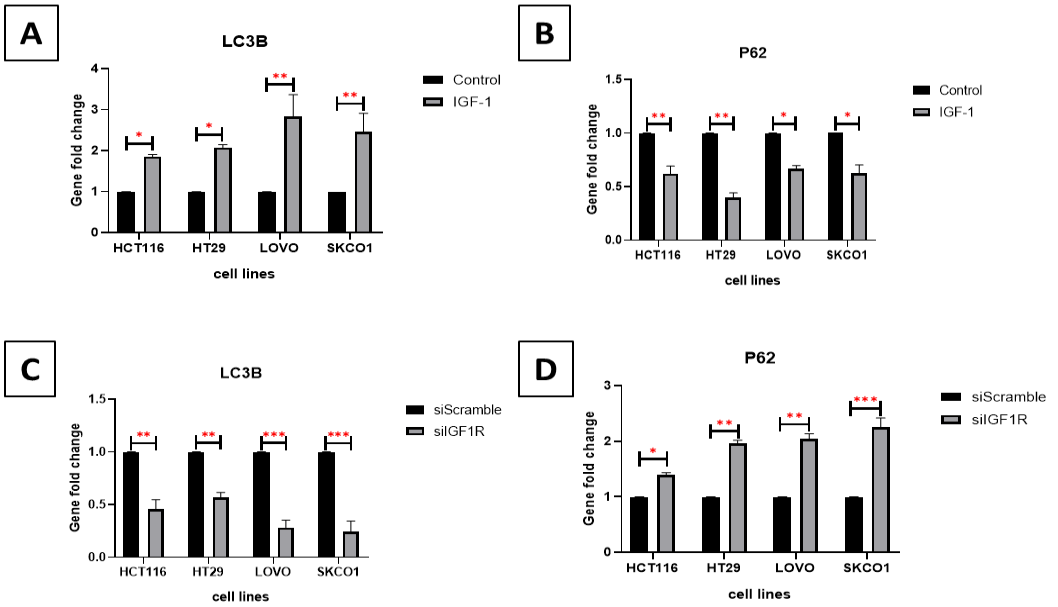
A
LC3B
Gene fold change
HCT116
HT29
LOVO
SKCO1
cell lines
Control
IGF-1
B
P62
Gene fold change
HCT116
HT29
LOVO
SKCO1
cell lines
Control
IGF-1
C
LC3B
Gene fold change
HCT116
HT29
LOVO
SKCO1
cell lines
siScramble
siIGF1R
D
P62
Gene fold change
HCT116
HT29
LOVO
SKCO1
cell lines
siScramble
siIGF1R

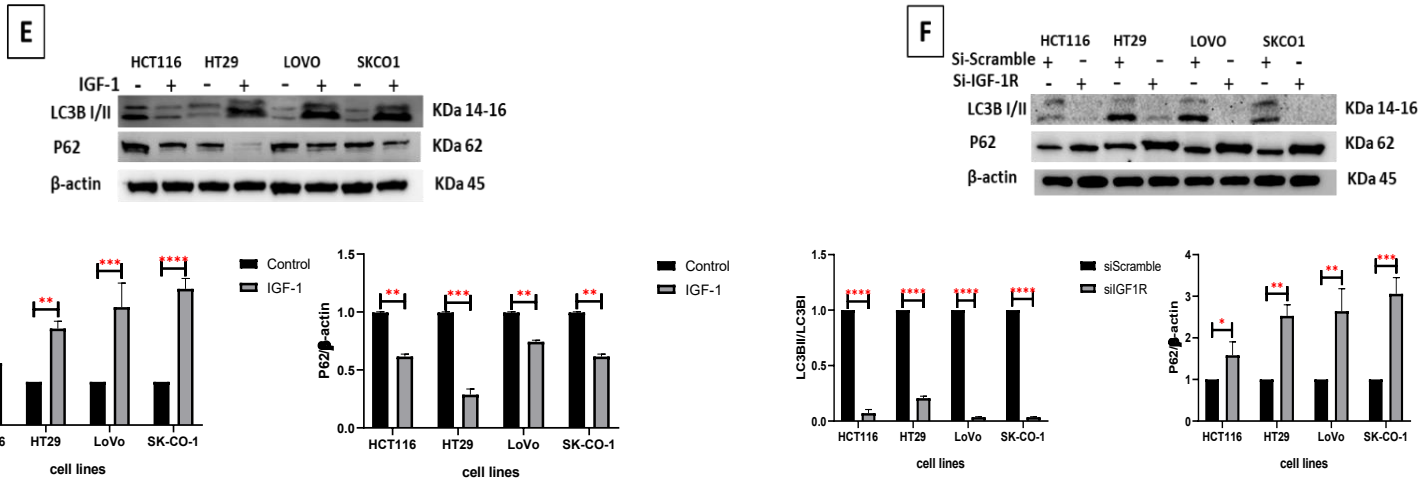
E
HCT116
HT29
LOVO
SKCO1
IGF-1
LC3B I/II
KDa 14-16
P62
KDa 62
β-actin
KDa 45
F
HCT116
HT29
LOVO
SKCO1
Si-Scramble
Si-IGF-1R
LC3B I/II
KDa 14-16
P62
KDa 62
β-actin
KDa 45

LC3BII/LC3BI
HCT116
HT29
LoVo
SK-CO-1
cell lines
Control
IGF-1
P62/β-actin
HCT116
HT29
LoVo
SK-CO-1
cell lines
Control
IGF-1

LC3BII/LC3BI
HCT116
HT29
LoVo
SK-CO-1
cell lines
siScramble
siIGF1R
P62/β-actin
HCT116
HT29
LoVo
SK-CO-1
cell lines
siScramble
siIGF1R

G

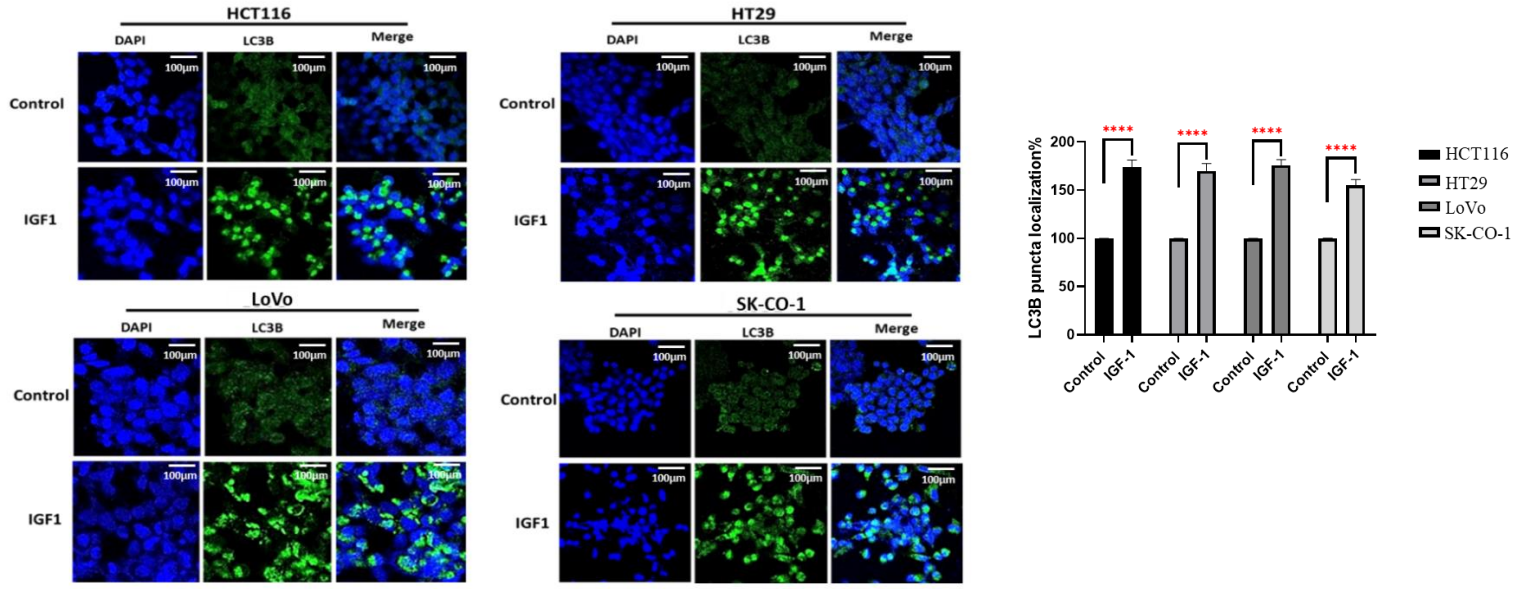
HCT116
HT29
LoVo
SK-CO-1
DAPI
LC3B
Merge
Control
IGF1
100μm
LC3B puncta localization%
Control
IGF-1
HCT116
HT29
LoVo
SK-CO-1

H

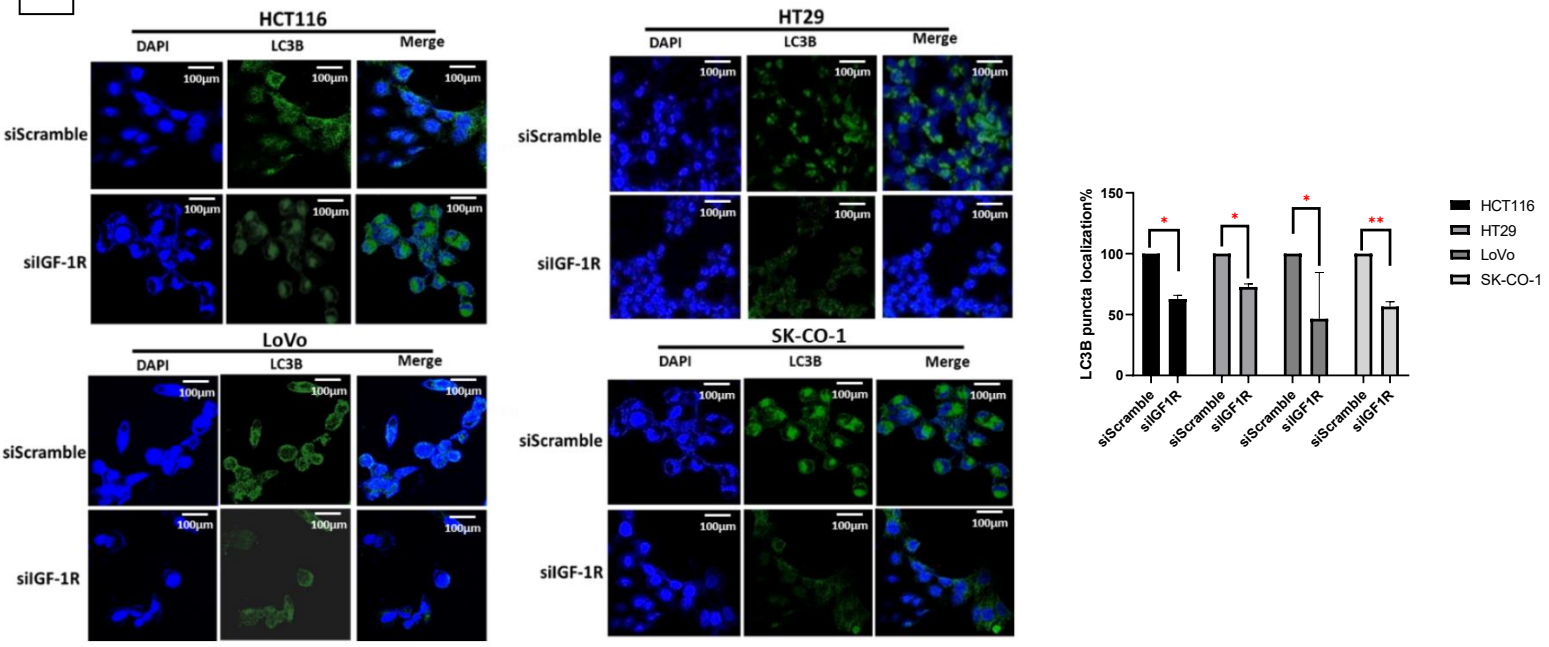
HCT116
HT29
LoVo
SK-CO-1
DAPI
LC3B
Merge
siScramble
siIGF-1R
100μm
LC3B puncta localization%
HCT116
HT29
LoVo
SK-CO-1

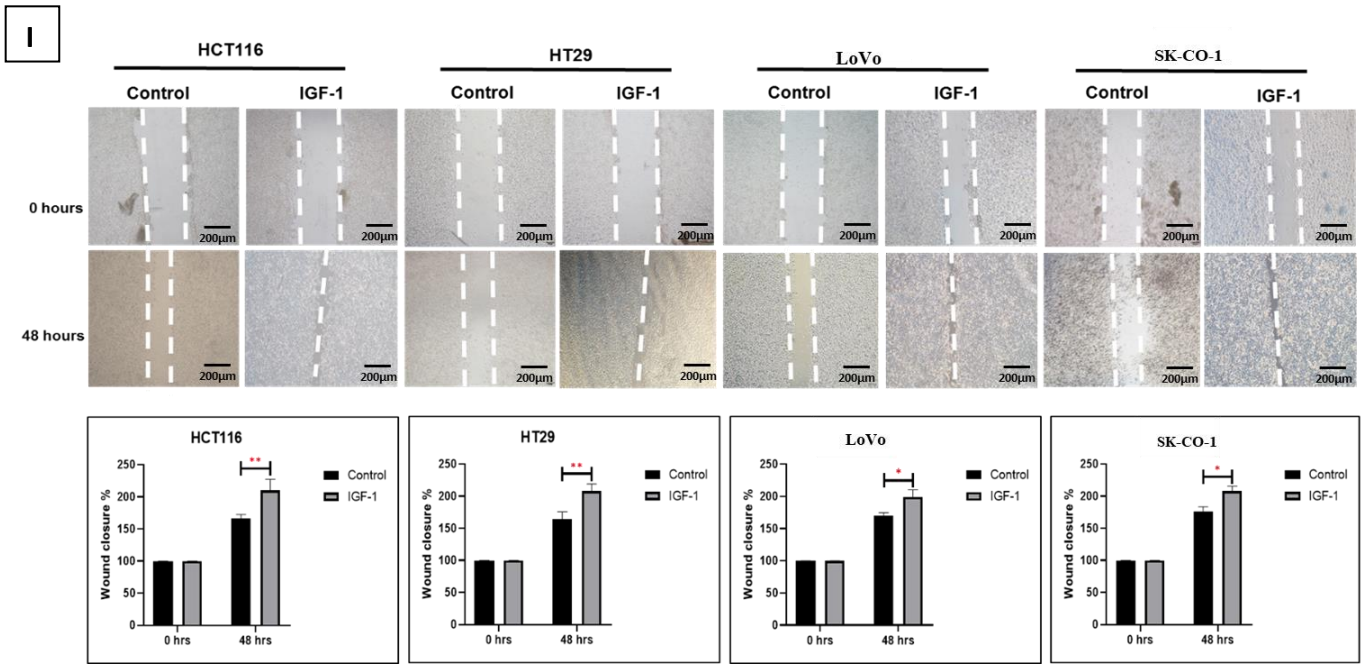

Figure 1: IGF-1-IGF-1R axis promotes autophagy and migration ability in CRC cells.

(A) LC3B mRNA expression in HCT116, HT29, LoVo, and SK-CO-1 cells in treated with IGF-1 normalized to untreated controls.
(B) P62 mRNA expression in HCT116, HT29, LoVo, and SK-CO-1 cells in treated with IGF-1 normalized to untreated controls.
(C) LC3B mRNA expression in HCT116, HT29, LoVo, and SK-CO-1 cells transfected with siIGF1R, normalized to siScramble controls.
(D) P62 mRNA expression in HCT116, HT29, LoVo, and SK-CO-1 cells transfected with siIGF1R, normalized to siScramble controls.

Protein levels of LC3BII and P62 in CRC cells HCT116, HT29, LoVo and SK-CO-1 in **(E)** control vs IGF-1 treatment, normalized to β-actin, **(F)** or siScramble vs siIGF1R, normalized to β-actin.

(G) Representative immunofluorescence images of autophagosome (LC3B puncta) and DAPI nuclear staining in control vs IGF-1 treatment in CRC cells: HCT116, HT29, LoVo and SK-CO-1.
(H) Representative immunofluorescence images of autophagosome (LC3B puncta) and DAPI nuclear staining in siScramble vs siIGF1R in CRC cells: HCT116, HT29, LoVo and SK-CO-1.
(I) The width of the scratch was noted at the pre-defined time points of 0 and 48 hours following IGF-1 treatment in CRC cell lines. Untreated cells were considered as a control, Cell cultures were measured at 0 and 48 h time points.
The values were compared across the different groups using a two-way ANOVA between the groups. $*$ $p < 0.05$, $**$ $p < 0.01$, $***$ $p < 0.001$ and $****$ $p < 0.0001$. Bars represent mean ± SD. Data were acquired from 3 replicas for the immunofluorescence stating and data were acquired from 3 different experiments for the wound healing assay. Original blots are presented in Figures S2 and S3.

2. Concurrent IGF-1R and autophagy inhibition reduces CRC cell migration and invasion.

Next, CRISPR/Cas9 gene editing technique has been used to knockout the autophagy genes, ATG5 or ATG7, to block conventional autophagy (Figure S4). Next, the levels of multiple autophagy-related proteins, including ATG5, ATG7 and LC3B have been evaluated in the HCT116, NC, ATG5-/- and ATG7-/- cell lines at protein levels (Figure 2A). The absent protein level of ATG5 in ATG5-/- and ATG7 protein level in ATG7-/- indicates effective knockout of both genes in HCT116 cell line upon CRISPR/Cas9 gene editing technique. Additionally, accumulation of LC3BI in ATG5-/- and ATG7-/- cell lines indicate defective autophagy due to the essential roles of ATG5 and ATG7 in LC3BI conversion as both ATG5 and ATG7 genes are required for LC3BI conversion to LC3BII.

Autophagy is contextual in metastasis, as it modulates cell migration through selective degradation of focal adhesion proteins and EMT. However, the specific role of IGF-1R in CRC migration and invasion remains poorly understood. Thus, at first IGF-1 treatment and silencing IGF-1R expression using siRNA has been performed on CRC cell lines, including HCT116, NC, ATG5-/- and ATG7-/-, and subsequently evaluated the efficacy of concurrent inhibition of IGF-1R and autophagy on cell migration. A scratch line was created in each well to assess cell migration, and migration was evaluated at predefined time points of 0 hours and 48 hours. HCT116 and NC cells treated with IGF-1 exhibited a higher migration rate compared to untreated cells after 48 hours, suggesting the ability of IGF-1 to promote cell migration (Figure 2B). However, HCT116 KO cell lines for ATG5 and ATG7 exhibited lower migration ability following IGF-1 treatment. IGF-1R knockdown via siRNA partially decreased parental cell lines HCT116 and NC migration ability (Figure 2C). Nevertheless, a significant decrease in the migration ability of both HCT116 KO cell lines treated with siRNA-IGF-1R was shown at 48hrs.

Following, a transwell invasion assay has been utilized to examine whether dual inhibition of autophagy and IGF-1R mitigates cell invasion (Figure 2D). IGF-1R knockdown via siRNA partially reduced the invasion of HCT116 and NC cells compared to their controls. However, dual inhibition of autophagy and IGF-1R in the KO cell lines significantly decreased cell invasion in both HCT116 KO cell lines compared to their controls.

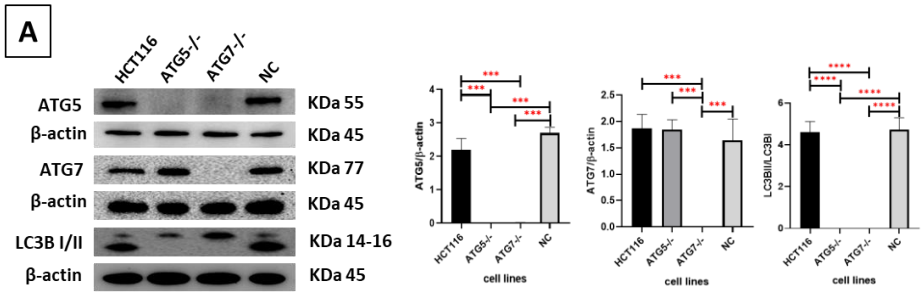

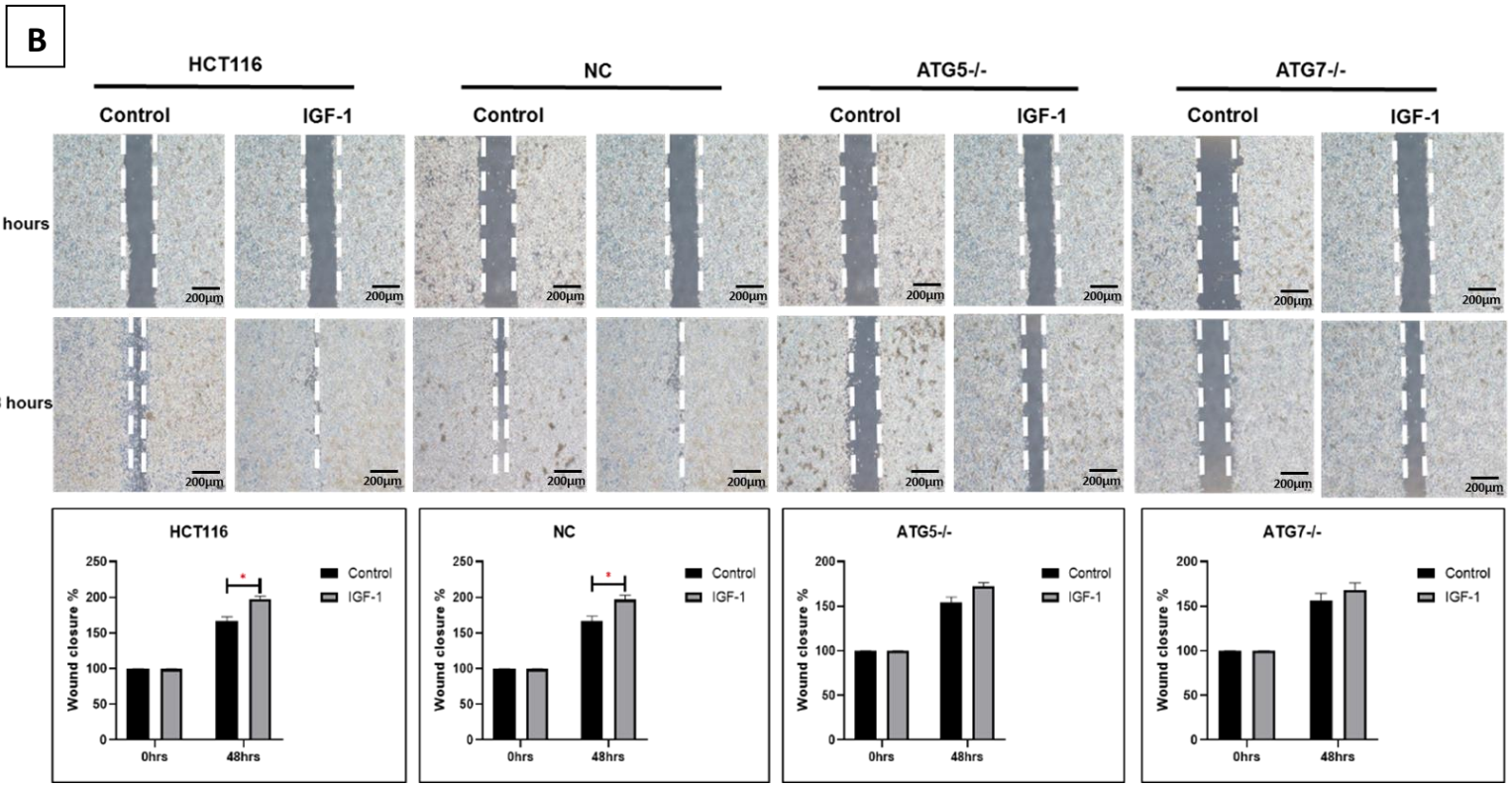
B
HCT116
NC
ATG5-/-
ATG7-/-
Control
IGF-1
0 hours
48 hours
200μm
Wound closure %
0hrs
48hrs
*

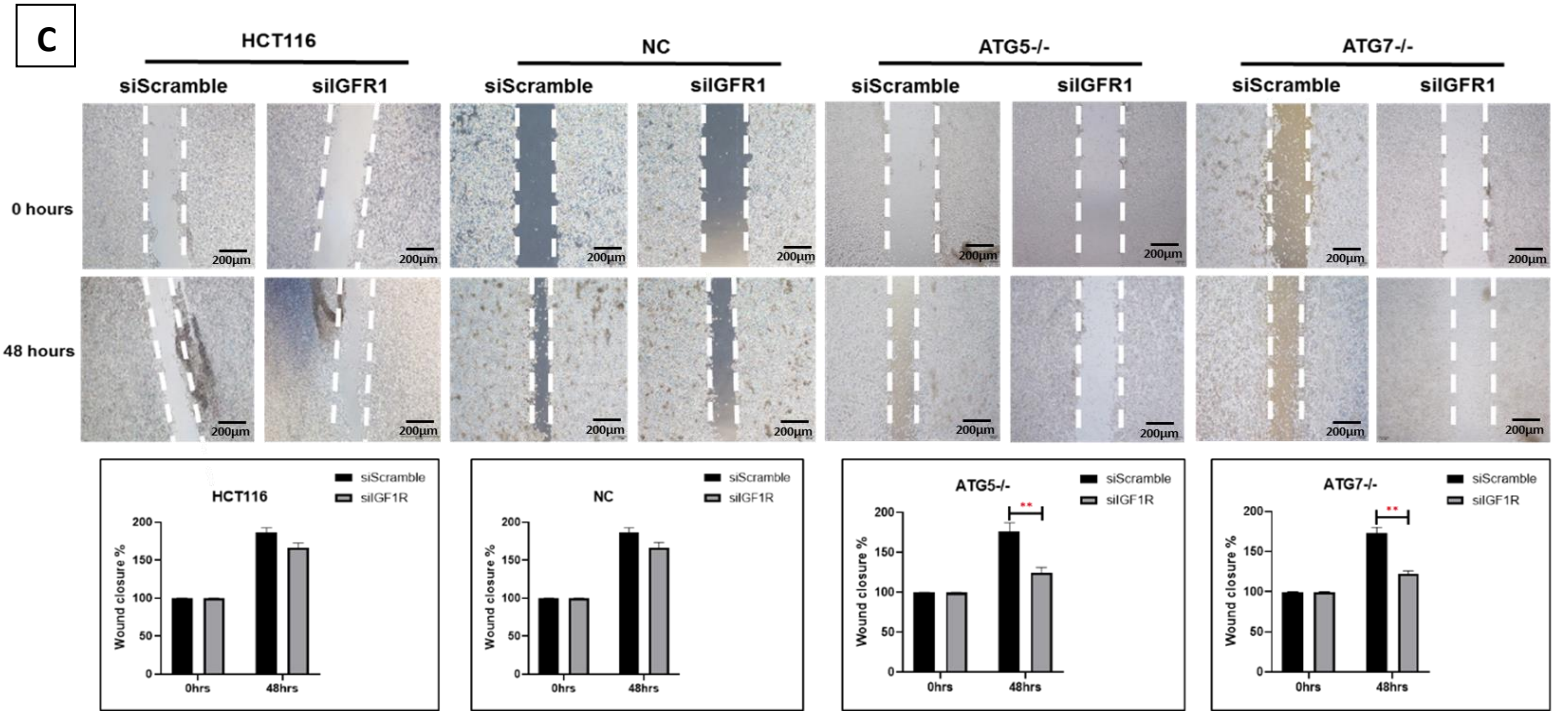
C
HCT116
NC
ATG5-/-
ATG7-/-
siScramble
siIGFR1
0 hours
48 hours
200μm
Wound closure %
0hrs
48hrs
**

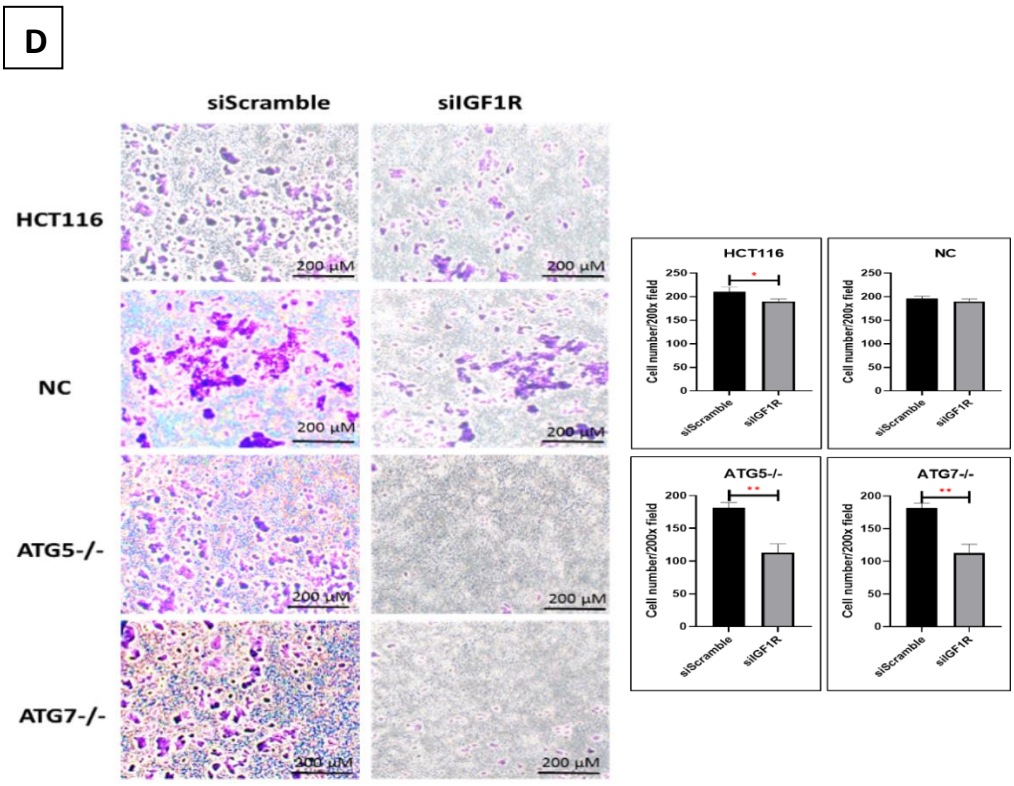

Figure 2: Dual inhibition of autophagy and IGF-1R reduces the migratory and invasion ability of CRC cells.

(A) Protein levels of LC3B, ATG5 and ATG7 in HCT116, NC, ATG5-/- and ATG7-/- Cell lines, normalized to β-actin.

(B) The width of the scratch was noted at the pre-defined time points of 0- and 48-hours following control vs IGF-1 treatment in parental HCT116 and NC vs HCT116 KO cell lines ATG5-/- and ATG7-/-,

(C) The width of the scratch was noted at the pre-defined time points of 0 and 48 hours following siScramble vs siIGF-1R in parental HCT116 and NC vs HCT116 KO cell lines ATG5-/- and ATG7-/-,

(D) Invasion assay shows the number of invaded cells in HCT116, NC, ATG5 KO and ATG7 KO cells following treatment with either siScramble or siIGF-1R.

The values were compared across the different groups using a two-way ANOVA between the groups or independent student's t-test between each two groups. $*$ $p < 0.05$, $**$ $p < 0.01$, $***$ $p < 0.001$ and $****$ $p < 0.0001$. Bars represent mean ± SD. Data were acquired from 3 different experiments in wound healing assay and from 3 different replicas in the invasion assay. Original blots are presented in Figure S5.

3. Bioinformatics analysis showed that IGF-1R expression is associated with activating epithelial-mesenchymal transition pathways.

A bioinformatics analysis was performed to gain further insights into the main pathways associated with the IGF-1-IGF-1R axis and underscore the overall role of IGF-1R in the pathogenesis of colorectal adenocarcinoma. Using Gene Set Cancer Analysis (GSCALite), we investigated the impact of IGF-1R on the activation or inhibition of cancer-related pathways. Figure 3A illustrates the percentage of colon adenocarcinoma cases in which the expression of the IGF-1R gene either activated (red) or inhibited (blue) specific pathways. Consistent with the transcriptomic analysis, our findings demonstrate that the IGF-1-IGF-1R axis is associated with the activation of EMT, which is known to contribute to invasion and migration in the later stages of CRC.

Furthermore, using the RNA-seq dataset from TCGA data in the UALCAN web tool, we evaluated the expression level of IGF-1R in different stages of colon adenocarcinoma [COAD] (Figure 3B). Consistent with transcriptomic analysis, we observed a significant upregulation of IGF-1R in late tumor stages (stage 3 compared to stages 1 and 2). Similarly, IGF-1R expression was significantly upregulated in late metastasis and lymph node stage in COAD (Figure 3C).

We also performed a Kaplan-Meier analysis using the GEPIA2 web tool to assess the overall survival based on CRC sample data. Notably, patients with high expression of IGF-1R exhibited a considerably poorer prognosis (Figure 3D). These findings underscore the potential significance of IGF-1R as a prognostic indicator in CRC.

A

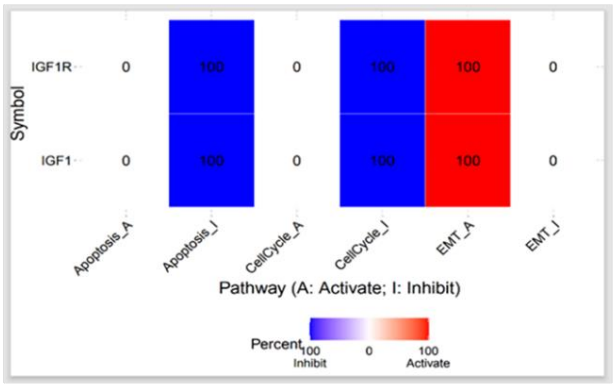

B

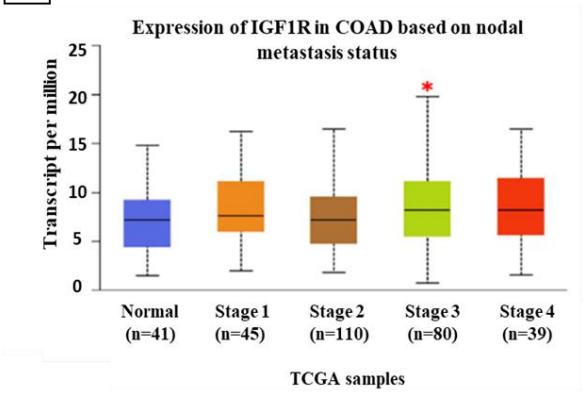

C

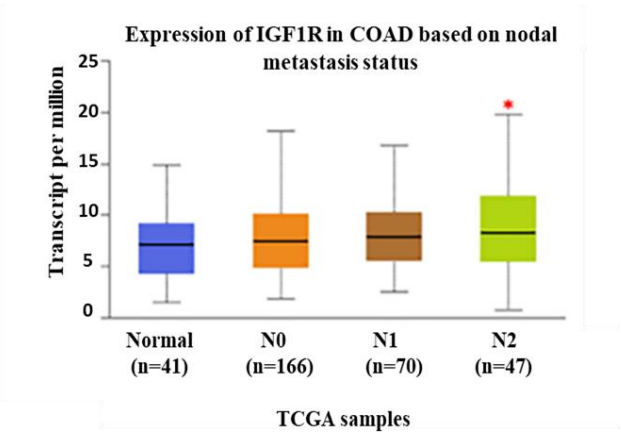

D

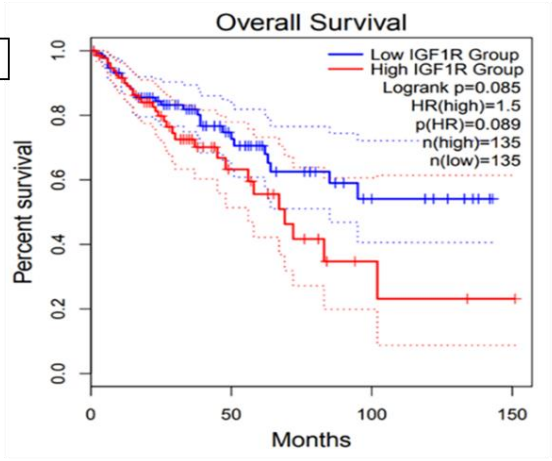

Figure 3: **Bioinformatics Analysis of IGF-1R role and expression in CRC.**

(A) Analysis of the Impact of IGF-1/IGF-1R Gene Expression on Pathway Activity in Colon Adenocarcinoma: A Summary Utilizing GSCALite and TCGA PanCancer COAD Datasets. The COAD-TCGA dataset included a total of 329 samples, comprising 288 tumor samples, 41 normal controls, and 26 paired samples.

(B) IGF-1R expression level in CRC stages. Using RNA seq dataset from TCGA data in UALCAN web tool, we compared the expression of IGF-1R in CRC stages. Student's t-test was calculated by the UALCAN web tool. * $p < 0.05$. Sample sizes for each group are indicated within the figure.

(C) IGF-1R expression level in CRC stages. Using RNA seq dataset from TCGA data in UALCAN web tool, we compared the expression of IGF-1R in Lymph node stage. Student's t-test was calculated by the UALCAN web tool. * $p < 0.05$. Sample sizes for each group are indicated within the figure.

(D) Kaplan-Meier analysis to assess the overall survival for CRC patients using the GEPIA2 web tool, which provides RNA seq from the TCGA data set. Sample sizes were n=135 for high IGF-1R expression and n = 135 for low expression. Statistical significance was evaluated using the log-rank (Mantel–Cox) test and hazard ratios (HRs) with 95% confidence intervals (CIs) were derived from Cox proportional-hazards regression analysis.

4. Concurrent IGF-1R and autophagy inhibition modulate EMT and Focal adhesion molecules in CRC cells.

Metastatic spread is initiated by EMT, which is essential for the initial phase of tumor cells spreading to distant organs. A critical event in EMT is the loss of E-cadherin expression. E-cadherin, a cell surface glycoprotein, facilitates intercellular adhesion by interacting with catenin through its extracellular and cytoplasmic domains. Downregulation of E-cadherin expression can destabilize cadherin/catenin complexes, leading to tumor migration and metastasis.

To gain mechanistic insight into the impact of concurrent IGF-1R and autophagy inhibition on CRC metastasis, next qPCR was performed to assess the mRNA expression levels of key EMT markers, including E-cadherin, Vimentin and Snail in CRC cell lines. In Figure 4A, our results demonstrated that siRNA-mediated knockdown of IGF-1R led to an upregulation of E-cadherin mRNA expression in HCT116 cell line. Notably, the ATG5-/- and ATG7-/- cell lines demonstrated a markedly enhanced upregulation of E-cadherin mRNA expression in siRNA-mediated knockdown of IGF-1R compared to the siScramble-treated controls. In contrast, Vimentin and Snail mRNA expressions, which are associated with enhanced tumor cell migration and invasion, were slightly downregulated in HCT116, with a more pronounced decrease observed in ATG5-/- and ATG7-/- cells (Figure 4B, C).

Flow cytometry analysis was conducted to further validate our results on the mRNA expression of different EMT markers to evaluate the levels of E-cadherin, Vimentin and Slug. In Figure 4D, Flow cytometry analysis demonstrated a slight increase in E-cadherin expression in HCT116 cells following IGF-1R knockdown compared to siScramble controls. In contrast, ATG5-/- and ATG7-/- cells showed significantly elevated E-cadherin levels under the same conditions. Additionally, Vimentin and Slug expression were significantly decreased in ATG5-/- and ATG7-/- cells after IGF-1R silencing (Figure 4E, F). These results indicate that combined inhibition of autophagy and IGF-1R signaling enhances epithelial characteristics and suppresses mesenchymal markers in CRC cells.

Focal adhesions (FAs) serve as extensive macromolecular complexes that connect the actin cytoskeleton and the extracellular matrix (ECM), facilitating traction. Properly regulated dynamics of focal adhesions play a crucial role in

cell migration. Immunofluorescence analysis targeting the focal adhesion proteins paxillin and zyxin demonstrated an augmentation in both the size and quantity of focal adhesions in autophagy-deficient cells transfected with siIGF-1R compared to parental HCT116 cells (Figure 4G-K). While paxillin is recruited early to nascent focal adhesions, zyxin is exclusively present in mature focal adhesions. This observation suggests that the heightened abundance and larger size of focal adhesions in autophagy-deficient cells indicate their mature state.

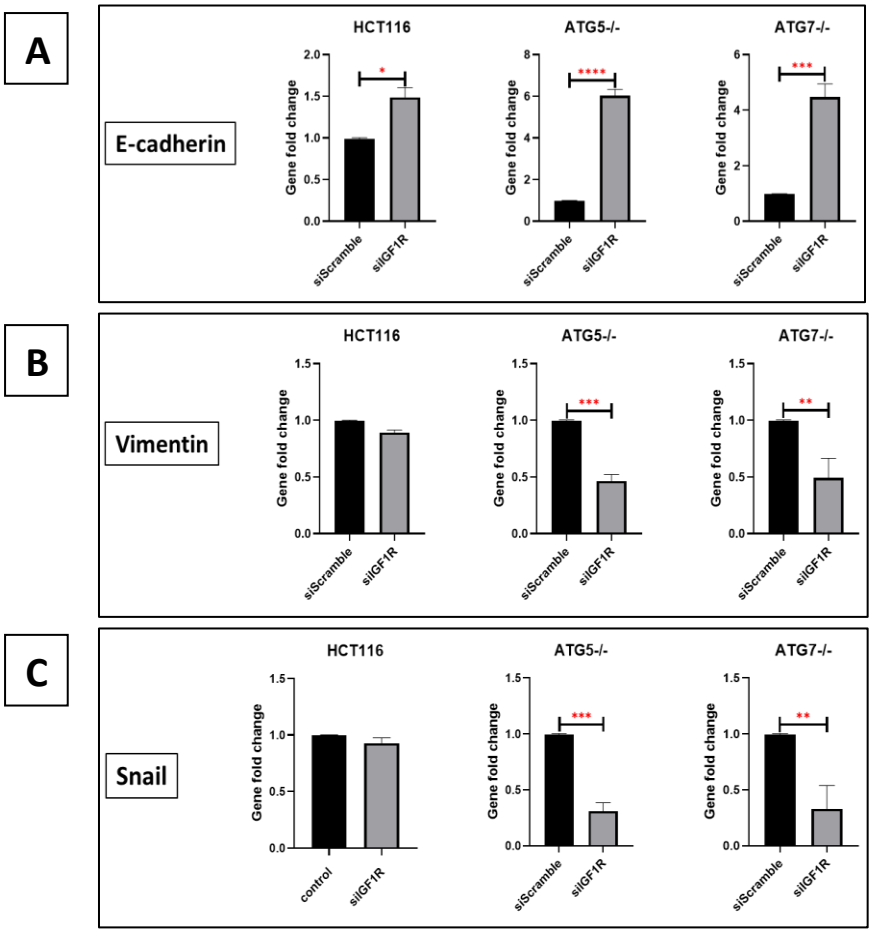

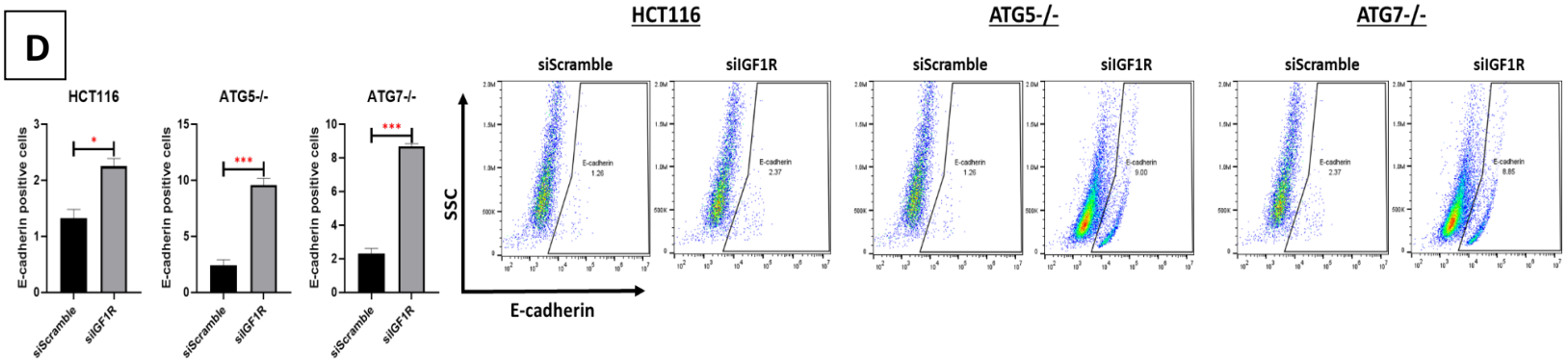

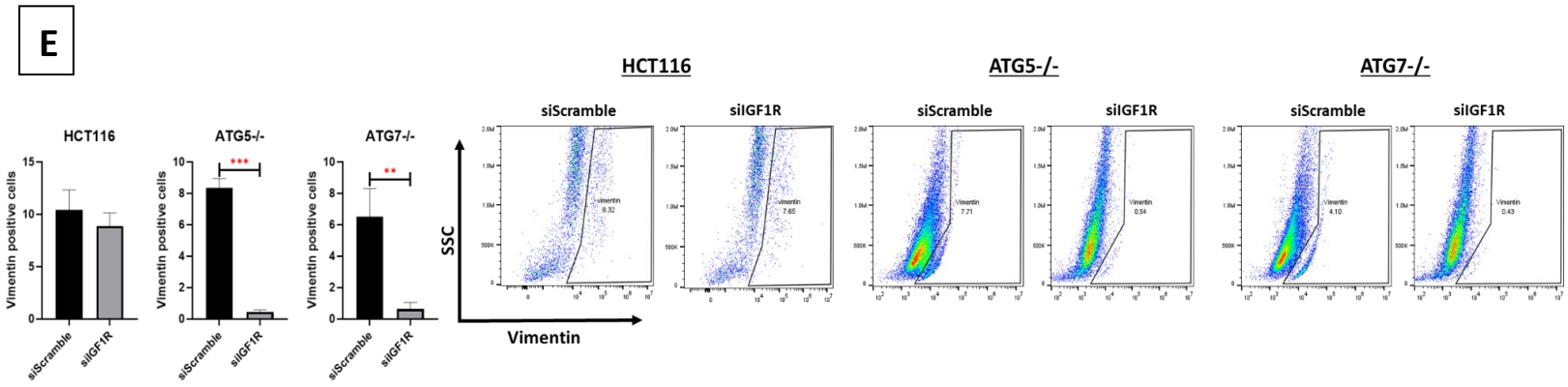
E
HCT116
ATG5-/-
ATG7-/-
Vimentin positive cells
siScramble
siIGF1R
***
**
HCT116
ATG5-/-
ATG7-/-
siScramble
siIGF1R
siScramble
siIGF1R
siScramble
siIGF1R
SSC
Vimentin

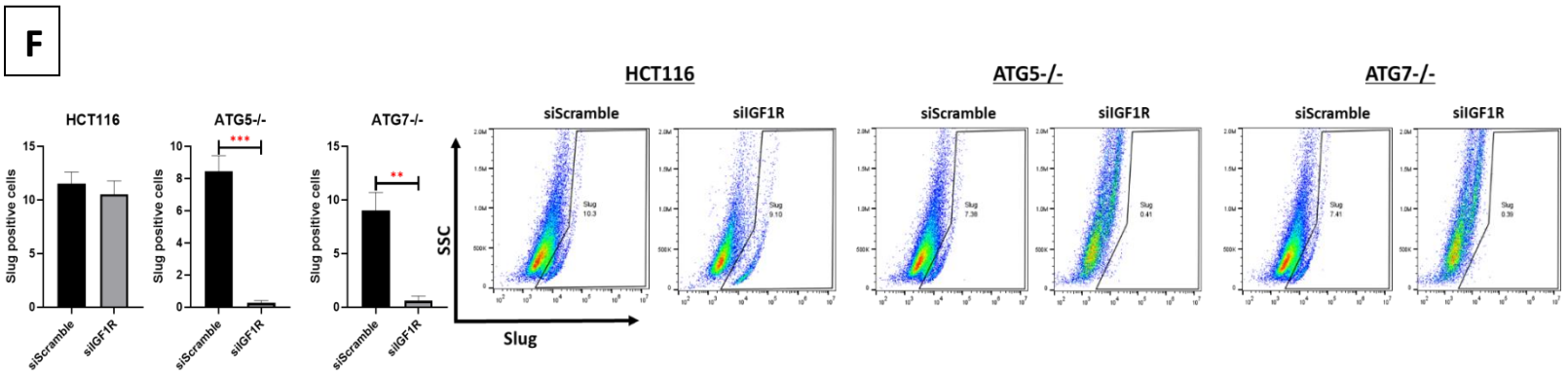
F
HCT116
ATG5-/-
ATG7-/-
Slug positive cells
siScramble
siIGF1R
***
**
HCT116
ATG5-/-
ATG7-/-
siScramble
siIGF1R
siScramble
siIGF1R
siScramble
siIGF1R
SSC
Slug

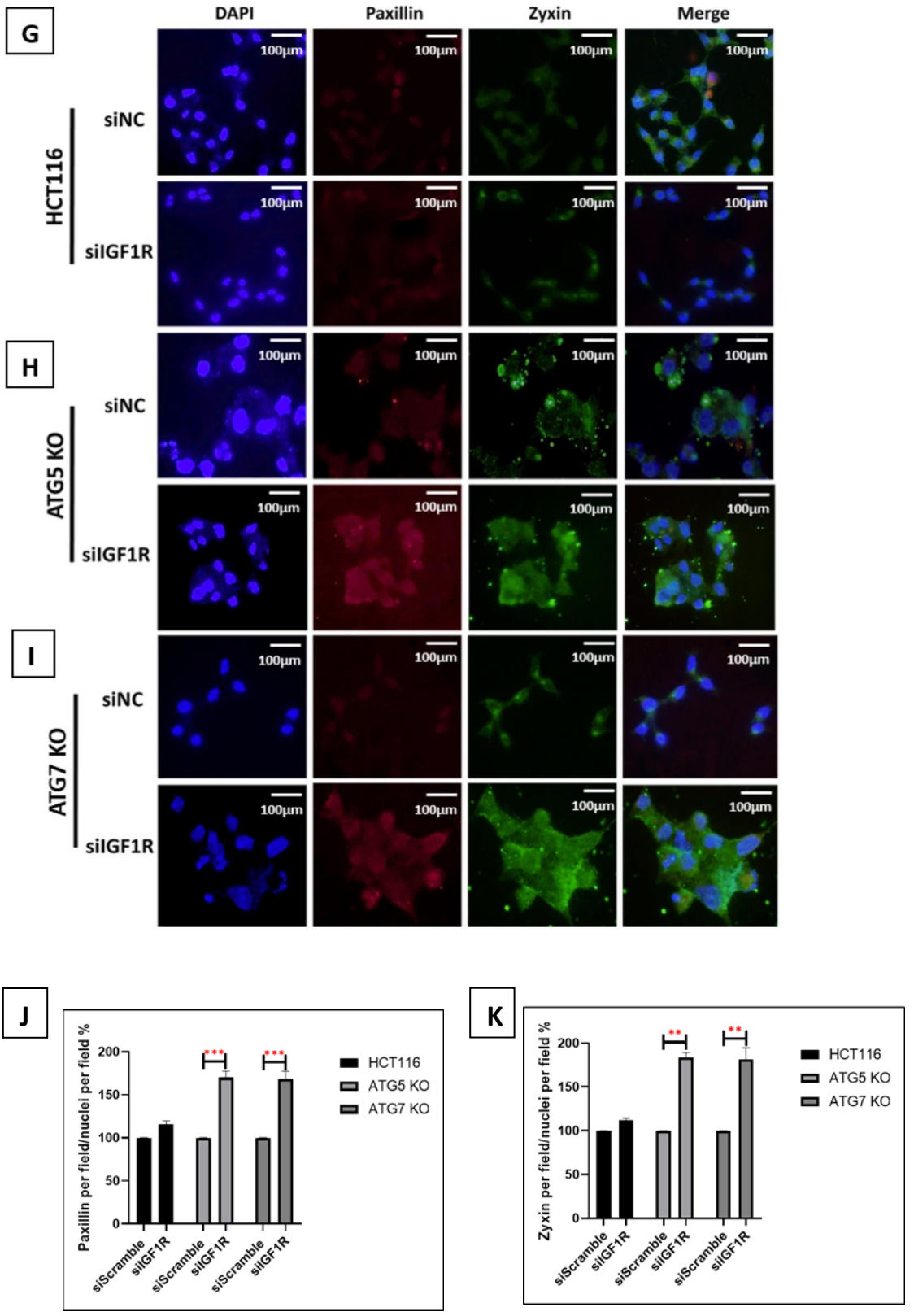
G
DAPI
Paxillin
Zyxin
Merge
HCT116
siNC
siIGF1R
100μm
H
ATG5 KO
siNC
siIGF1R
I
ATG7 KO
siNC
siIGF1R
J
Paxillin per field/nuclei per field %
200
150
100
50
0
***
***
siScramble
siIGF1R
siScramble
siIGF1R
siScramble
siIGF1R
HCT116
ATG5 KO
ATG7 KO
K
Zyxin per field/nuclei per field %
200
150
100
50
0
**
**
siScramble
siIGF1R
siScramble
siIGF1R
siScramble
siIGF1R
HCT116
ATG5 KO
ATG7 KO

Figure 4: Dual inhibition of autophagy and IGF-1R modulates EMT markers and focal adhesion molecules levels.

qPCR analysis of mRNA expression of EMT markers **(A)** E-cadherin, **(B)** Vimentin and **(C)** Snail, in HCT116, ATG5-/- and ATG7-/- cells transfected with siIGF-1R, normalized to siScramble controls. Flow cytometry analysis of EMT markers **(D)** E-cadherin, **(E)** Vimentin and **(F)** Slug in CRC cell lines following IGF-1R knockdown by siRNA compared to siScramble controls. Representative immunofluorescence images of paxillin, zyxin and DAPI nuclear staining in siScramble vs siIGf-1R treatment in CRC cells **(G)** HCT116, **(H)** ATG5-/- and **(I)** ATG7-/-**. (J)** Quantification of Paxillin colocalization in siScramble vs siIGF-1R in HCT116, ATG5-/- and ATG7-/-**. (K)** Quantification of Zyxin colocalization in siScramble vs siIGF-1R in HCT116, ATG5-/- and ATG7-/-.

The values were compared across the different groups using a two-way ANOVA and independent student's t-test. $*$ $p < 0.05$, $**$ $p < 0.01$, $***$ $p < 0.001$ and $****$ $p < 0.0001$. Bars represent mean ± SD. Data were acquired from 3 different experiments in qPCR and from 3 replicas in immunofluorescence staining.

Discussion

Based on our previous transcriptomics analysis of FFPE patient samples from different stages of CRC [20], we identified autophagy pathways and the IGF-1R gene as top differentially expressed genes in the advanced stage compared to early CRC stages (I and II). In this study, CRISPR-Cas9 technology has been utilized to knock out the autophagy-related genes ATG5 and ATG7 in the HCT116 CRC cell line. Our results demonstrated increased autophagy flux following IGF-1 treatment, as evidenced by the elevated levels of LC3II isoform. Conversely, silencing IGF1R suppressed autophagy flux. Furthermore, the combined inhibition of IGF-1R and autophagy reduced CRC cell migration. We observed significant downregulation of the EMT markers Vimentin, Snail, and Slug, while E-cadherin significantly increased in ATG5-/- and ATG7-/- cell lines. These findings collectively indicate a potent modulation of EMT markers in CRC cells when both IGF-1R and autophagy are concurrently inhibited. Our results highlight a novel potential therapeutic approach targeting CRC metastasis by combining IGF-1R inhibition and autophagy suppression.

Autophagy plays an important role in CRC progression and therapy resistance, as cancer cells utilize autophagic activity to sustain metabolic needs and survival. Starvation-induced autophagy promotes invasion, migration, and EMT marker expression in CRC cells, an effect induced by rapamycin and reversed by Beclin-1 knockdown [27].

Numerous studies have demonstrated that the inhibition of IGF1R exerts distinct effects on autophagy in cancer cells. A large-scale compound screening identified picropodophyllotoxin as an IGF1R inhibitor that not only activates autophagy but also plays a crucial role in enhancing chemotherapy-induced immunogenic cell death [28]. Conversely, Renna et al. demonstrated that IGF-1R silencing reduced autophagosome formation in HeLa cells via inhibition of mTORC2 and subsequent reduction of PKC α/β activity [29]. Consistent with this latter mechanism, our data show that IGF-1R knockdown reduces autophagy flux, supporting a regulatory role for IGF-1R in autophagic activity.

Extensive evidence supports the involvement of the IGF-1/IGF-1R axis in CRC initiation and metastasis. IGF-1R is frequently overexpressed in CRC and correlates with clinical features such as venous invasion and liver metastasis [30]. Furthermore, Reinmuth N et al. emphasized IGF-1R as a legitimate target for treating human colon cancer, as it is implicated in various pathways that regulate the growth, angiogenesis, and metastasis of colon cancer [31, 32]. Amplified IGF-1/IGF-1R signaling has also been linked to CRC cell survival, invasion, metastasis, and resistance to chemotherapy [33-36]. Colorectal carcinomas have been found to exhibit IGF-I and -II levels higher than those in adjacent healthy colonic mucosa [13]. Notably, the liver, the most common site of colorectal cancer metastasis, is the primary source of IGF-1. In gastric cancer, the co-expression levels of IGF-1R and multidrug resistance-associated protein-1 (MRP-1) in the tumor have been shown to help predict the effectiveness of chemotherapy [37]. Moreover, IGF-1R expression has been associated with a worse prognosis lymph node metastases and serves as an independent predictor of survival in patients [37].

Several agents targeting the IGF pathway have been investigated for treating CRC based on the well-recognized pro-tumorigenic role of IGF-1. Although figitumumab monotherapy did not yield clinical benefit in metastatic CRC [38], the combination therapy of the IGF inhibitor BMS-754807 with receptor tyrosine kinase inhibitors, such as cetuximab, showed a potentiated effect of the latter [39]. Similarly, a promising therapeutic approach demonstrated both in vitro and in vivo involves the combined inhibition of IGF-1R (using agents such as linsitinib or figitumumab) and MEK1/2 (with inhibitors like U0126 or selumetinib), which together exert synergistic anti-proliferative effects across various colorectal cancer cell lines and xenograft models [40].

Additionally, a few studies have investigated the combination of IGF-1R and autophagy inhibitors in various solid tumors, yielding promising results in suppressing tumor proliferation. For example, in triple-negative breast cancer cell lines MDA-MB-231 and BT-549, employing a combination of the IGF-1R inhibitor NVP-AEW541 and the autophagy inhibitor 3-MA revealed similar outcomes [41]. Another study found that targeting IGF1R together with ERK enhances the effectiveness of autophagy inhibitors in pancreatic ductal adenocarcinoma (PDAC) cells [42]. These findings highlight the potential tumor-suppressing benefits of targeting IGF-1R and autophagy pathways in solid tumors. Our results provide proof of concept for the combined effect of IGF-1R and autophagy in promoting the metastasis of colorectal cancer and highly suggest the potential therapeutic role of the combined blockade to prevent and/or suppress metastasis.

Focal Adhesion (FA) molecules constitute extensive macromolecular assemblies facilitating the establishment of mechanical linkage between the actin cytoskeleton and the extracellular matrix. The finely regulated dynamics of FA are essential for governing cellular migration processes [43]. Autophagy plays a pivotal role in modulating the motility and invasive properties of highly metastatic tumor cells by regulating the turnover of FA molecules [44, 45]. Perturbation of autophagic activity in metastatic tumor cells leads to the accumulation of paxillin, a key component of FA, consequently impeding the disassembly of FA complexes, cell spreading, and cellular motility [44]. The interaction between processed LC3 and paxillin is facilitated through a conserved LIR motif located in the amino-terminal region of paxillin, which is modulated by oncogenic Src activity.

Finally, our bioinformatics analysis using publicly available web tools provided additional insights into the role of the IGF-1-IGF-1R axis in CRC progression. Gene Set Cancer Analysis (GSCALite) revealed that the IGF-1-IGF-1R axis is associated with the activation of EMT. Moreover, analysis of the RNA-seq dataset from TCGA data demonstrated a significant upregulation of IGF-1R expression in late metastatic stages of CRC. These findings were biologically validated by our experimental results, providing further support for the critical role of IGF-1R in CRC metastasis and emphasizing its potential as a promising therapeutic target for colon cancer.

A plausible explanation for the observed link between IGF-1R signaling, autophagy modulation, and EMT may involve the PI3K/Akt and Ras/Raf/ERK pathways, which are known drivers of EMT through transcriptional activation of Snail, Slug, ZEB, and Twist, ultimately repressing E-cadherin and promoting mesenchymal transition [46]. Concurrently, the PI3K/Akt/mTOR axis is a central negative regulator of autophagy initiation, creating a regulatory interface where IGF-1R–dependent signaling and autophagy may intersect. In tumor cells under metabolic or oncogenic stress, this relationship can become more complex, with autophagy paradoxically increasing to support metastatic survival [47, 48]. In parallel, the Ras/Raf/ERK cascade represents an important convergence point: activated ERK promotes EMT-related transcriptional programs [49], while oncogenic Ras can induce autophagy to maintain metabolic fitness in nutrient-limited environments [50]. Notably, blocking autophagy has been shown to reverse EMT in Ras-mutant cancer cells, underscoring the reliance of this phenotype on autophagic support. While our dual-inhibition findings are consistent with the possibility that these pathways converge downstream of IGF-1R, we cannot rule out additional intermediates or parallel mechanisms. Therefore, further studies are needed to define the precise molecular nodes that coordinate IGF-1R activity, autophagy regulation, and EMT progression.

Conclusion

In conclusion, this study demonstrates that dual inhibition of autophagy flux and insulin-like growth factor 1 (IGF-1) signaling, achieved through genetic or pharmacological approaches, markedly suppresses colorectal cancer (CRC) cell migration and epithelial–mesenchymal transition (EMT) marker expression. These findings highlight the therapeutic potential of co-targeting IGF-1R and autophagy pathways to limit metastatic progression in CRC. However, as the current evidence is derived solely from in vitro assays, further in vivo studies are warranted to validate these translational implications and assess their clinical relevance.

Acknowledgments

We would like to acknowledge our patients, who voluntarily provided the samples for the initial transcriptomics analysis.

Funding

This research was funded by MBRU-AlMahmeed Research Award, 2019 (ALM#1914).

Conflict of Interest

No conflict of interest.

Ethics Approval

The studies involving human participants were reviewed and approved by the Research Ethics Committee, University of Sharjah (Ref. No.: REC-17-11-23-01). Written informed consent for participation was not required for this study in accordance with the national legislation and the institutional requirements. The study was conducted according to the principles of the Declaration of Helsinki of 1975 (revised 1983).

Consent for publication

The early transcriptomic analysis was retrospectively conducted on FFPE blocks; the Research Ethics Committee waived the need for patients' consent.

Authors Contribution

Eglal Mahgoub: Wrote and prepared the manuscript. **Khuloud Bajbouj:** for experimental work and data analysis. **Samrein Ahmed:** for CRISPR-Cas9 gene editing experiments and data analysis. **Shirin Hafezi:** for experimental work and data analysis. **Leen Eldohaji:** for experimental work and data analysis. **Thenmozhi Venkatachalam:** for bioinformatics analysis. **Mahmood Hachim:** for bioinformatics analysis. **Tasneem Al Hamidi:** for experimental work and data analysis. **Jasmin Shafarin:** for experimental work and data analysis. **Wael M. Abdel-Rahman:** visualization and revision. **Nabil Sulaiman:** visualization and revision. **Rifaat Hamoudi:** Bioinformatics Analysis and revision. **Jalal Taneera:** visualization and revision. **Ritu Lakhtakia:** visualization and revision. **Iman M. Talaat:** Patient recruitment, data collection and Revision. **Maha Saber-Ayad:** responsible for the conception of the idea, visualization and revision. All authors approved the manuscript.

Data Availability

All data generated or analyzed during this study are included in this published article [and its supplementary information files].

References

1. Bray, F., et al., *Global cancer statistics 2022: GLOBOCAN estimates of incidence and mortality worldwide for 36 cancers in 185 countries.* CA: a cancer journal for clinicians, 2024. **74**(3): p. 229-263.
2. Chen, Y., et al., *Global colorectal cancer screening programs and coverage rate estimation: an evidence synthesis.* Journal of Translational Medicine, 2025. **23**(1): p. 811.
3. Bromham, N., et al., *Colorectal cancer: summary of NICE guidance.* Bmj, 2020. **368**.
4. Guo, L., et al., *Transactivation of Atg4b by C/EBPβ promotes autophagy to facilitate adipogenesis.* Molecular and cellular biology, 2013. **33**(16): p. 3180-3190.
5. White, E. and R.S. DiPaola, *The double-edged sword of autophagy modulation in cancer.* Clinical cancer research, 2009. **15**(17): p. 5308-5316.
6. Boya, P., F. Reggiori, and P. Codogno, *Emerging regulation and functions of autophagy.* Nature cell biology, 2013. **15**(7): p. 713-720.
7. White, E., *Deconvoluting the context-dependent role for autophagy in cancer.* Nature reviews cancer, 2012. **12**(6): p. 401-410.
8. Degenhardt, K., et al., *Autophagy promotes tumor cell survival and restricts necrosis, inflammation, and tumorigenesis.* Cancer cell, 2006. **10**(1): p. 51-64.
9. Polyak, K. and R.A. Weinberg, *Transitions between epithelial and mesenchymal states: acquisition of malignant and stem cell traits.* Nature Reviews Cancer, 2009. **9**(4): p. 265-273.
10. Nieto, M.A., et al., *EMT: 2016.* Cell, 2016. **166**(1): p. 21-45.
11. Zheng, L., et al., *Metabolic syndrome: molecular mechanisms and therapeutic interventions.* Molecular Biomedicine, 2025. **6**(1): p. 59.
12. Demir, A.N., et al., *The Metabolic Syndrome: A Cancer Risk Factor?* Journal of Experimental and Basic Medical Sciences, 2023. **4**(1): p. 012-020.
13. Chen, Z. and Q. Hong, *Correlation of serum IGF-1, AGEs and their receptors with the risk of colorectal cancer in patients with type 2 diabetes mellitus.* Frontiers in Oncology, 2023. **13**: p. 1125745.
14. Chang, C. and C. Ulrich, *Hyperinsulinaemia and hyperglycaemia: possible risk factors of colorectal cancer among diabetic patients.* Diabetologia, 2003. **46**(5): p. 595-607.
15. Hagiwara, A., M. Nishiyama, and S. Ishizaki, *Branched-chain amino acids prevent insulin-induced hepatic tumor cell proliferation by inducing apoptosis through mTORC1 and mTORC2-dependent mechanisms.* Journal of cellular physiology, 2012. **227**(5): p. 2097-2105.
16. Durai, R., et al., *The role of the insulin-like growth factor system in colorectal cancer: review of current knowledge.* International journal of colorectal disease, 2005. **20**(3): p. 203-220.
17. Kawaguchi, T., et al., *Branched-chain amino acid-enriched supplementation improves insulin resistance in patients with chronic liver disease.* International journal of molecular medicine, 2008. **22**(1): p. 105-112.
18. Lum, J.J., et al., *Growth factor regulation of autophagy and cell survival in the absence of apoptosis.* Cell, 2005. **120**(2): p. 237-248.
19. Soori, M., G. Lu, and R.W. Mason, *Cathepsin inhibition prevents autophagic protein turnover and downregulates insulin growth factor-1 receptor–mediated signaling in neuroblastoma.* The Journal of pharmacology and experimental therapeutics, 2016. **356**(2): p. 375-386.
20. Talaat, I.M., et al., *Evaluation of galanin expression in colorectal cancer: an immunohistochemical and transcriptomic study.* Frontiers in Oncology, 2022. **12**: p. 877147.
21. Zhang, S., et al., *Strategies in the delivery of Cas9 ribonucleoprotein for CRISPR/Cas9 genome editing.* Theranostics, 2021. **11**(2): p. 614.

22. Vanamala, J., et al., *Resveratrol suppresses IGF-1 induced human colon cancer cell proliferation and elevates apoptosis via suppression of IGF-1R/Wnt and activation of p53 signaling pathways.* BMC cancer, 2010. **10**: p. 1-14.
23. Collins, T.J., *ImageJ for microscopy.* Biotechniques, 2007. **43**(sup1): p. S25-S30.
24. Liu, C.-J., et al., *GSCALite: a web server for gene set cancer analysis.* Bioinformatics, 2018. **34**(21): p. 3771-3772.
25. Chandrashekar, D.S., et al., *UALCAN: a portal for facilitating tumor subgroup gene expression and survival analyses.* Neoplasia, 2017. **19**(8): p. 649-658.
26. Tang, Z., et al., *GEPIA2: an enhanced web server for large-scale expression profiling and interactive analysis.* Nucleic acids research, 2019. **47**(W1): p. W556-W560.
27. Shen, H., et al., *Knockdown of Beclin-1 impairs epithelial-mesenchymal transition of colon cancer cells.* Journal of Cellular Biochemistry, 2018. **119**(8): p. 7022-7031.
28. Wu, Q., et al., *Autophagy induction by IGF1R inhibition with picropodophyllin and linsitinib.* Autophagy, 2021. **17**(8): p. 2046-2047.
29. Renna, M., et al., *IGF-1 receptor antagonism inhibits autophagy.* Human molecular genetics, 2013. **22**(22): p. 4528-4544.
30. Oshima, T., et al., *Clinicopathological significance of the gene expression of matrix metalloproteinase-7, insulin-like growth factor-1, insulin-like growth factor-2 and insulin-like growth factor-1 receptor in patients with colorectal cancer: insulin-like growth factor-1 receptor gene expression is a useful predictor of liver metastasis from colorectal cancer.* Oncology reports, 2008. **20**(2): p. 359-364.
31. Li, H., et al., *IGF-IR signaling in epithelial to mesenchymal transition and targeting IGF-IR therapy: overview and new insights.* Molecular cancer, 2017. **16**(1): p. 6.
32. Marcucci, F., P. Ghezzi, and C. Rumio, *The role of autophagy in the cross-talk between epithelial-mesenchymal transitioned tumor cells and cancer stem-like cells.* Molecular cancer, 2017. **16**(1): p. 3.
33. Zhang, C., et al., *Elevated IGFIR expression regulating VEGF and VEGF-C predicts lymph node metastasis in human colorectal cancer.* BMC cancer, 2010. **10**(1): p. 184.
34. Zhu, X., et al., *Biomarkers of lymph node metastasis in colorectal cancer: update.* Frontiers in Oncology, 2024. **14**: p. 1409627.
35. Vigneri, P.G., et al., *The insulin/IGF system in colorectal cancer development and resistance to therapy.* Frontiers in oncology, 2015. **5**: p. 230.
36. Kasprzak, A., *Autophagy and the insulin-like growth factor (IGF) system in colonic cells: implications for colorectal neoplasia.* International journal of molecular sciences, 2023. **24**(4): p. 3665.
37. Ge, J., et al., *Expression levels of insulin-like growth factor-1 and multidrug resistance-associated protein-1 indicate poor prognosis in patients with gastric cancer.* Digestion, 2009. **80**(3): p. 148-158.
38. Becerra, C.R., et al., *Figitumumab in patients with refractory metastatic colorectal cancer previously treated with standard therapies: a nonrandomized, open-label, phase II trial.* Cancer chemotherapy and pharmacology, 2014. **73**: p. 695-702.
39. Carboni, J.M., et al., *BMS-754807, a small molecule inhibitor of insulin-like growth factor-1R/IR.* Molecular cancer therapeutics, 2009. **8**(12): p. 3341-3349.
40. Flanigan, S.A., et al., *Overcoming IGF1R/IR resistance through inhibition of MEK signaling in colorectal cancer models.* Clinical cancer research, 2013. **19**(22): p. 6219-6229.
41. Wu, W., et al., *Co-targeting IGF-1R and autophagy enhances the effects of cell growth suppression and apoptosis induced by the IGF-1R inhibitor NVP-AEW541 in triple-negative breast cancer cells.* PLoS One, 2017. **12**(1): p. e0169229.

42. Stalnecker, C.A., et al., *Concurrent inhibition of IGF1R and ERK increases pancreatic cancer sensitivity to autophagy inhibitors.* Cancer research, 2022. **82**(4): p. 586-598.
43. Parsons, J.T., A.R. Horwitz, and M.A. Schwartz, *Cell adhesion: integrating cytoskeletal dynamics and cellular tension.* Nature reviews Molecular cell biology, 2010. **11**(9): p. 633-643.
44. Sharifi, M.N., et al., *Autophagy promotes focal adhesion disassembly and cell motility of metastatic tumor cells through the direct interaction of paxillin with LC3.* Cell reports, 2016. **15**(8): p. 1660-1672.
45. Ridley, A.J., *Life at the leading edge.* Cell, 2011. **145**(7): p. 1012-1022.
46. Hua, H., et al., *Insulin-like growth factor receptor signaling in tumorigenesis and drug resistance: a challenge for cancer therapy.* Journal of hematology & oncology, 2020. **13**(1): p. 64.
47. Amaravadi, R.K., et al., *Principles and current strategies for targeting autophagy for cancer treatment.* Clinical cancer research, 2011. **17**(4): p. 654-666.
48. Kocak, M., et al., *Targeting autophagy in disease: established and new strategies.* Autophagy, 2022. **18**(3): p. 473-495.
49. Tripathi, K. and M. Garg, *Mechanistic regulation of epithelial-to-mesenchymal transition through RAS signaling pathway and therapeutic implications in human cancer.* Journal of cell communication and signaling, 2018. **12**(3): p. 513-527.
50. Schmukler, E., Y. Kloog, and R. Pinkas-Kramarski, *Ras and autophagy in cancer development and therapy.* Oncotarget, 2014. **5**(3): p. 577.